ANALYSIS OF CNS LYMPHATIC SYSTEMS OF C57BL/6 AND SJL MICE POST-INFECTION WITH THEILER'S VIRUS

An Undergraduate Research Scholars Thesis

by

CONNOR JOHNSON

Submitted to the Undergraduate Research Scholars program at
Texas A&M University
in partial fulfillment of the requirements for the designation as an

UNDERGRADUATE RESEARCH SCHOLAR

Approved by Research Advisor: Dr. C. Jane Welsh

May 2017

Major: Biomedical Sciences

TABLE OF CONTENTS

TABLE OF FIGURES

Page

ABSTRACT

Analysis of CNS Lymphatic Systems of C57BL/6 and SJL Mice Post-Infection with Theiler's Virus

Connor Johnson
Department of Neuroscience
Texas A&M University

Research Advisor: Dr. C. Jane Welsh
Department of Veterinary Integrative Biosciences
Texas A&M University

Theiler's Murine Encephalomyelitis Virus (TMEV) infection is an important murine model for epilepsy and multiple sclerosis, however, it does not affect all mouse strains equally. SJL and C57BL/6 mice can both be infected with the BeAn strain of TMEV and experience the initial encephalitic phase. C57BL/6 mice develop seizures during the first week of infection and then clear the virus from the CNS, however, infected SJL mice do not develop seizures, are unable to clear the virus, and develop a chronic immune-mediated demyelinating disease similar to multiple sclerosis. One factor that may contribute to these different disease phenotypes may be the newly discovered CNS lymphatic system. To test this hypothesis, the two strains of mice will be infected with TMEV and comparisons will be made of the lymphatic systems found in the dura mater surrounding their brains. Expression of the chemoattractant CCL21 as well as the lymphatic system's morphology will be observed through immunofluorescence microscopy to determine any differences. Any large differences between the two strains could help to elucidate why C57BL/6 mice are resistant to the demyelinating phase while SJL mice are not, a critical question in understanding the TMEV multiple sclerosis model.

DEDICATION

I would like to dedicate this paper to my family and friends, who have helped me to push myself do my best throughout my life and continue to do so daily.

ACKNOWLEDGEMENTS

I would like to acknowledge Megha, Colin, and Rae's help with this experiment. I could not have done it without your (near constant) help and expertise, and I have no idea where I would be in this project without y'all!

Additionally, I would like to acknowledge Felix Lu and his help with the dissections of the meninges, since it saved more than a couple of them from getting shredded. I would also like to thank him and Dr. Li for letting me borrow their dissecting microscope and for helping me with the initial staining, as these proved to be immensely useful in the dissections.

I would also like to thank my family for encouraging me on my work in research and for being understanding, even when I was working on the project over the break!

Finally, I would like to thank Dr. Welsh for her help on basically every step of this project, and for being my mentor for this project. You were there whenever I had any questions, and you helped me avoid many mistakes during this project. Whether it was terminations during one of the busiest times of the year, or just looking through the thesis and making sure I made as few mistakes as possible, you have been incredibly helpful.

ABBREVIATIONS

CCL21	Chemokine (C-C motif) ligand 21
CCR7	C-C chemokine receptor type 7
CNS	Central Nervous System
PI	Principal Investigator
TMEV	Theiler's Murine Encephalomyelitis Virus
MS	Multiple Sclerosis
BSA	Bovine Serum Albumin
b.w.	Body Weight
p.i.	Post Infection
MOG	Myelin-oligodendrocyte glycoprotein

SECTION I

INTRODUCTION

Theiler's Murine Encephalomyelitis virus

Theiler's virus, or TMEV, is the name of a group of related picornaviruses that can be found in the central nervous systems of mice and can cause a persistent inflammatory disease similar to multiple sclerosis (MS) in susceptible strains of mice.[1] There are various subgroups and strains of TMEV, and this experiment focuses on the BeAn strain of the virus that is part of the less virulent TO subgroup. This strain causes a sub-lethal encephalitis similar to polioencephalomyelitis followed by persistent infection in white matter of the spinal cord, making the persistent/chronic phase of the virus a very good model for MS.[2] Certain strains of mice, C57BL/6 specifically, can also develop seizures during the early acute stage. However, epileptic-like seizures are not observed in other strains, such as the SJL. The chronic demyelinating stage is known as Theiler's virus-induced demyelinating disease (TMEV-IDD, abbreviated to TVID).[3] TMEV-IDD is not found in resistant strains such as C57BL/6. This strain is able to clear the virus after the acute stage and do not experience the MS-like symptoms seen in SJL mice.[4]

This difference in viral persistence is curious, because its cause is not fully known. There are various factors both in the virus and the mouse that can contribute to it, and it is likely a combination of these factors plus those yet to be discovered that are the ultimate cause of this viral persistence. One factor, viral plaque size, could be a determinant of viral persistence. A variant of the virus with a smaller plaque has been shown to be more able to cause the chronic demyelinating phase of the virus in those mice that are susceptible.[5] The mouse MHC class type

is very important in determining the resistance of a strain of mouse to chronic persistence. Mice with the B10 (H-2b), B10.D2 (H-2d), or B10.K (H-2k) MHC haplotype are resistant to virus-induced demyelination, and this resistance is passed down as a dominant trait.[6] Other genes are also involved in resistance and susceptibility to viral persistence, and there are likely other circumstances yet to be discovered that could affect this that could also affect the chronic stage of the disease.

Lymphatic Vasculature

The lymphatic system, part of the circulatory and immune systems, serves to channel the flow of a substance known as lymph that carries immune cells like lymphocytes and macrophages.[7] It runs alongside the circulatory system in most places, however, certain organs in which it would be disadvantageous to have an inflammatory immune response do not have connections to the immune system. One example of an immune privileged organ is the eye, where it would be disadvantageous to have an inflammatory response due to presence of an antigen because this response could lead to impairment of vision. This immune privilege is largely caused by a lack of lymphatic drainage through classical lymphatic vasculature that reduces the number of lymphocytes and inflammatory cells in the eye.[8]

The brain is another site of immune privilege, thought to be due in part to lack of lymphatic drainage. However, a new paper has recently proved this to be untrue as the authors discovered lymphatic vasculature in the meninges surrounding the brain.[9] This new vasculature has been found along the transverse and superior sagittal sinuses, and well as other areas in the meninges inferior to the brain.[10] It has been carefully characterized and imaged using

microscopic imaging techniques in order to fully view the extent of this new vasculature. This lymphatic vasculature had remained hidden until very recently due to advances in imaging, such as immunofluorescence and scanning confocal microscopy, and the fact that this vasculature is small, difficult to see, and is often overlooked due to its proximity to the major sinuses of the brain. However, given its location, it likely plays an important role in regulating the immune activity of the central nervous system.

Lymphatic Vasculature and Disease

The lymphatic system, being part of the immune system, plays a large role in actively combating infections that may come about during the disease. For example, lymphatic endothelial cells can secrete substances like cytokine (C-C motif) ligand 21 (CCL21), one of the main markers of the activated lymphatic system examined in the current study. CCL21, when expressed by lymphatic endothelial tissue, can bind to a chemokine receptor known as CCR7. This receptor plays a significant role in recruiting dendritic cells, T lymphocytes, and B lymphocytes across endothelial venules.[11] Since CCL21 is a chemoattractant, one would expect increased numbers of immune cells attracted to the areas where it is more highly expressed in lymphatic vascular tissue.

Chemotaxis of lymphocytes such as T lymphocytes towards CCL21 is an aspect of diseases like multiple sclerosis, and reduced chemotaxis towards CCL21 has been linked with a reduction of scores of myelin-oligodendrocyte glycoprotein (MOG)-induced EAE.[12] MS, being an autoimmune disorder, involves expression of multiple different chemokines throughout the immune system in order to cause demyelination. This demyelination, similar to that found in

susceptible strains of TMEV-infected mice, may also have some action involving chemokines, specifically CCL21. Given that CCL21 is expressed by lymphatic endothelial tissue, the newly discovered cerebral lymphatic system may play a role in the progression of diseases such as Theiler's virus and the susceptibility of certain mice to demyelination. However, there is no current research discussing the differences, if any, between the morphology and CCL21 expression of CNS lymphatic tissue between SJL and C57BL/6 mice after infection with TMEV. Any differences between the CNS lymphatic systems of these two mice could play a significant role in determining why C57BL/6 mice are able to clear the virus while SJL mice are unable to.

SECTION II

METHODS

Housing and Infection

In this experiment, twenty female mice were used from Harlan/Envigo: 10 SJL and 10 C57BL/6. The mice were caged in groups of 4 and allowed to acclimate to their new environment for about two weeks. Weight and behavioral data were collected once a day six days prior to injection and twice a day for seven days after injection. Eight mice from each strain were injected intracranially with BeAn strain of TMEV. The other two mice from each group were kept as controls and given a sham injection in the same location with a phosphate-buffer solution. Mice were terminated at day 7 p.i.

Termination and Dissection of the Meninges

Termination was carried out seven days after injection for each group. Each mouse was euthanized with Beuthanasia-D special pentobarbital (Schering-Plough Animal Health) via an intraperitoneal injection. The dissection and staining procedures were performed according to the procedure outlined in a recent paper characterizing meninges published by Louveau et al.[8] Mice were perfused with an ice-cold 10 mls of 0.1M PBS solution through the left ventricle of the heart. After perfusion, mice were decapitated and the skin and flesh was removed from the skull. The optic nerves were severed to remove the eyes, then the large muscles at the mandibular junction were severed to remove the lower jaw from the skull. After this, the lower orbits of the skull (maxillae, zygomatic, and squamosae) were removed. All flesh was cleaned from the skull, after which the nasal bone was removed using a coronal cut along its most caudal suture. A cut was then made around the skull inferior to the posttympanic hook, and this section of the skull

was then removed. The brain and lower skull were discarded. The skullcap was then placed into a 24-well plate with about 1 ml of a fixation solution made up of 0.1M PBS and 4% PFA and left to fix overnight.

After fixing overnight, the skullcaps were washed with PBS three times for five minutes each time. The skullcap was then placed in a petri dish containing PBS under a dissecting microscope. The meninges were scored around the edge of the interior of the skullcap using a Dumont #5 forceps. After scoring, the meninges were then removed by holding onto the transverse and superior sagittal sinus and carefully pulling them off. Skullcap and all other items that were not the meninges in the petri dish were discarded, and the meninges were left in the PBS petri dish until the immunostaining step.

Immunostaining

Meninges were then removed from the PBS petri dish and mounted onto a glass slide. The PBS solution was drained from them, and then incubated with a blocking solution containing 2% of either bovine serum albumin or goat serum and 0.1% Triton-X-100 in 0.1M PBS for 1 h at room temperature. The blocking solution was then removed and each meninge was incubated with a solution of the properly diluted primary antibodies: either goat anti-mouse Lyve-1 (eBioscience, clone ALY7, 1:200) or anti-CCL21 (R&D systems, AF457, 1:100). This incubation occurred overnight at 4^{o} C in PBS containing 1% BSA and 0.5% Triton-X-100. The mounts were then washed three times for 5 minutes with room temperature PBS. They were then incubated in a properly diluted solution of either goat anti-rat IgG FITC (Serotec, 1:1000) or bovine anti-goat IgG (Sigma-Aldrich, 1:1000) for 1 h at room temperature in a PBS solution

containing 1% BSA and 0.5% Triton-X-100. The solution was then removed from the slide, and a PBS solution containing 1:2000 Hoescht stain was added and incubated for 10 minutes at room temperature. The meninges were then washed, and a coverslip was placed on the slide and secured with Flouromount to finally mount the slide.

Imaging

Each slide was then imaged using an Olympus Vanox AHBS3 fluorescence microscope at 4x magnification. Multiple images were taken with the microscope to encompass the entire area of each meninge using a camera attachment and SPOT software. Each image was then overlaid with either a blue DAPI filter (for the Hoescht stain), a red filter (for the Lyve-1), or a green filter (for the CCL21) depending on what light source was used to fluoresce the sample. For some meninges, the Hoescht stain image and the Lyve-1 or CCL21 images were merged using SPOT. These images were then assembled into a mosaic depicting the entire meninge using Adobe Photoshop CS6 provided by the Texas A&M Student Computing Center. If the meninges had any notable structures or characteristics, these were imaged as well at varying magnifications to better display any significant characteristics, and were arranged in a similar fashion to the whole-mount images.

SECTION III

RESULTS AND DISCUSSION

Weight Recordings Before and After Infection

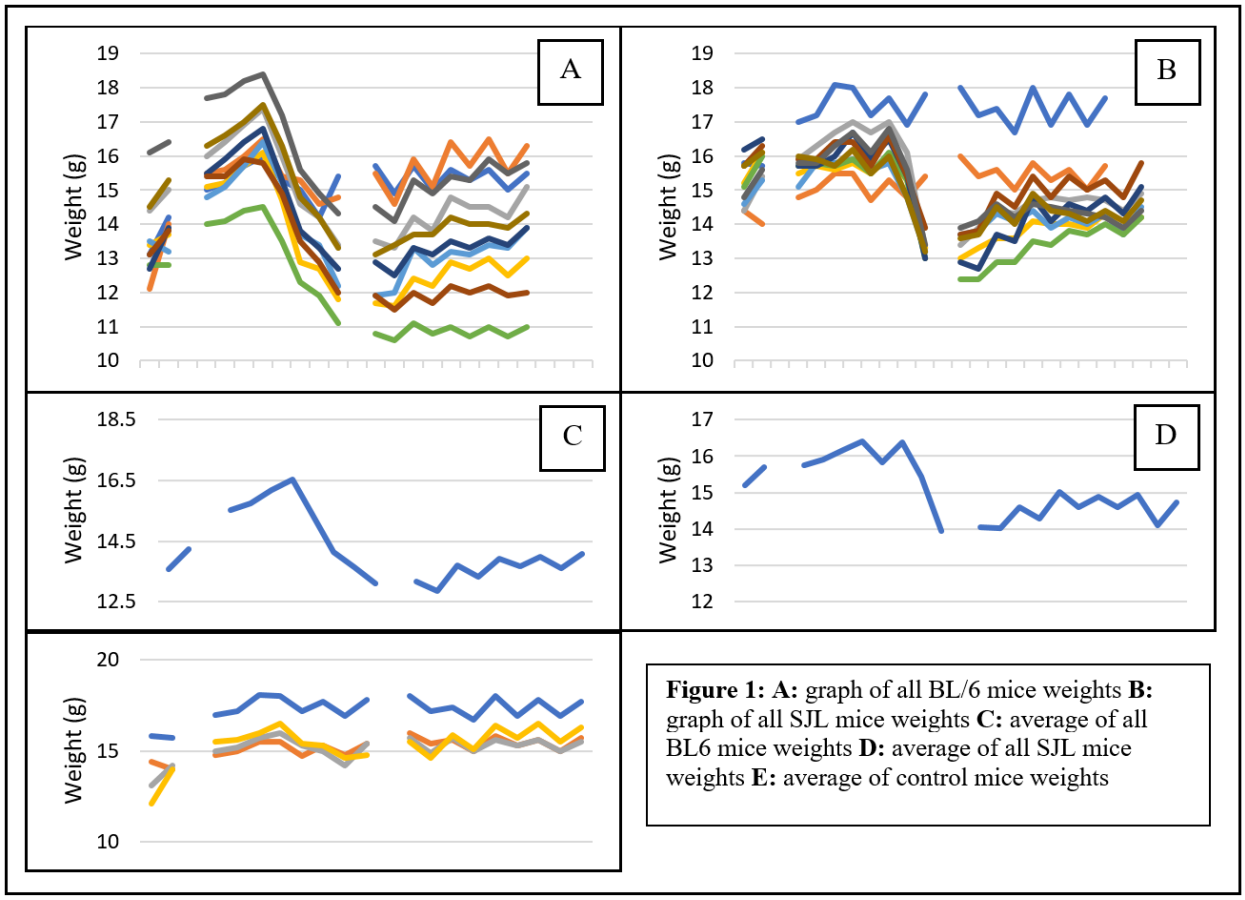

Figure 1: A: graph of all BL/6 mice weights **B:** graph of all SJL mice weights **C:** average of all BL6 mice weights **D:** average of all SJL mice weights **E:** average of control mice weights

Mice were weighed once a day pre-infection and twice per day post-infection to ensure that infection was successful. Infection was deemed to be successful if the mouse experienced a significant weight loss within a day of injection. All experimental mice met this criteria (Fig. 1a,b), while the control mice did not (Fig. 1e). The time of infection is clearly shown in Fig. 1a-d for all of the experimental mice by the dramatic weight loss found in the graph. The control mice were infected at the same time, but as evidenced by Fig. 1a,b,e, they did not experience the same weight loss as the experimental mice infected with TMEV.

The graphs of the BL/6 and SJL mouse averages show a sharp decrease in weights immediately after infection (Fig. 1c,d). This weight loss is characteristic of infection with TMEV, and demonstrates that the experimental mice, even those who did not exhibit seizures post-infection, were infected with the virus. The control mice, however, did not exhibit any noticeable decrease in weight before or after the saline injection. (Fig. 1e). The change in the weight of the infected mice along with the lack of any noticeable decrease in mouse weight in the control mice fits established symptoms of TMEV infection.[13]

Despite the initial weight loss, mouse weights in both infected groups stabilized about 3 days p.i. and then slowly started gaining weight (Fig. 1c,d). This trait is also consistent with the established symptoms of TMEV infection.[13] Mice in both the SJL and BL/6 groups maintained their weight or gained a slight amount of weight 3-7 days p.i. until they were terminated.

Behavior Recording of Mice Post-Infection

Mouse														
1			ND											
2			ND											
3			ND											
4			ND											
5			ND											
6			ND											
7			ND											
8			ND											
9			ND											
10			ND				5							
11			ND											
12			ND											
13			ND					5	4					
14			ND			4	4		5		5			
15			ND	2			4							
16			ND											
17			ND			5	5		5	5				
18			ND							5				
19			ND	1	1				5	5	3			
20			ND		5	5	5							

Racine Scores: 1, 2, 3, 4, 5

Figure 2: chart of Racine scores for all mice for each observation after infection. ND is no data. Mice 1-10 were SJL, mice 11-20 were BL/6. Mice 1, 2, 11, and 12 were the controls. Black squares are after mice were terminated.

Mouse behavior was also recorded post-infection to observe seizures characteristic of BeAn TMEV infection in C57BL/6 mice. Each mouse was scored daily using the Racine scale, which classifies seizures into five stages, or scores: 1: mouth and facial movements. 2: head nodding. 3: forelimb clonus. 4: rearing. 5: rearing and falling. Additionally, a full motor seizure is also classified as a stage 5 seizure.[15] As expected, Fig. 2 shows that 87.5% of the experimental BL/6 mice exhibited seizures that scored at least a 4, and 75% exhibited at least one full motor seizure. These seizures, characteristic of TMEV infection in C57Bl/6mice, show that the disease did progress in the animals as expected. The one BL/6 mouse that did not exhibit seizures still exhibited post-ictal behavior during some observations, so it likely experienced multiple seizures when unobserved, like the other BL/6 mice.

An interesting note is that one of the SJL mice experienced a seizure as well (Fig. 2), something not usually seen in SJL mice. Infection of SJL mice with Theiler's virus typically does not induce epilepsy, only the demyelinating disease later on in life.[16] However, one of the SJL mice in this experiment did exhibit at least one seizure. The mouse exhibited some of the same symptoms as the infected BL/6 mice, namely, weight loss and ataxia. Since this seizure does not fit previously established phenomena, there could be some experimental error causing it instead. Rarely, cross-breeds between susceptible strains of mice and resistant strains of mice, such as a BL/6 x SJL hybrid, can experience epilepsy following infection.[13] It is possible the intra-cerebral injection may have caused the seizure as a result of trauma from the injection, but none of the control mice exhibited any epileptic activity or weight loss (Fig. 1a,b) despite following the same injection procedure as the experimental mice. The seizure also occurred around the same time as the seizures in the infected BL/6 mice (Fig. 2), further increasing the likelihood that it was due to viral infection.

Additionally, two of the BL/6 mice exhibited ataxia and possibly some minor paralysis in their hind limbs. Their ataxia is likely due to nerve damage similar as the virus infects motor neuron cells during this stage of infection.

Meningeal Lyve-1 Expression

Analysis of Meninges

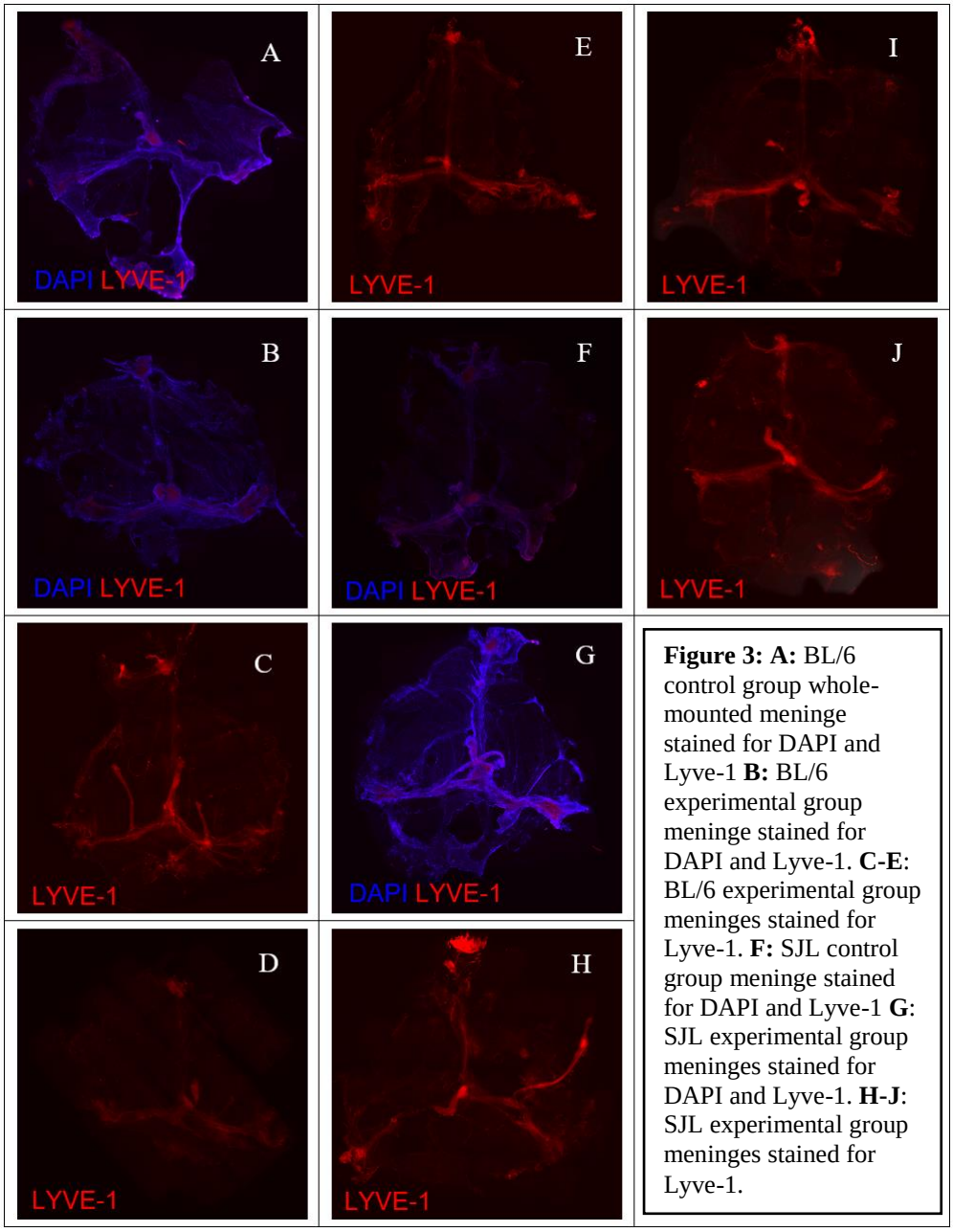

Figure 3: A: BL/6 control group whole-mounted meninge stained for DAPI and Lyve-1 **B:** BL/6 experimental group meninge stained for DAPI and Lyve-1. **C-E**: BL/6 experimental group meninges stained for Lyve-1. **F:** SJL control group meninge stained for DAPI and Lyve-1 **G**: SJL experimental group meninges stained for DAPI and Lyve-1. **H-J**: SJL experimental group meninges stained for Lyve-1.

Meninges were successfully stained for Lyve-1 to display lymphatic endothelial markers (Fig 3a-j). Most of this expression was observed in the sagittal and transverse sinuses of the dura mater, as expected by previously established findings.[9,10] Meninges in both strains of mice

expressed Lyve-1 markers seemingly evenly, with minor differences between each slide. The confluence of the sinuses stained very strongly in both the control and experimental mice. The confluence of sinuses and the sections of the transverse sinus approaching the base of the cranium were the only other heavily stained sections of the lymphatic network in the control mice. This increased staining approaching the lymphatics of the basal cranium is consistent with previously observed phenomena as shown by Aspelund et al.[10]

In the experimental mice, increased expression of Lyve-1 was observed along the entirety of the transverse and sagittal sinuses, when present (Fig. 3b-e, g-j). While removing the meninges, some were damaged with tears, holes, or missing sections of sinus. Despite these errors, the meningeal lymphatic networks in the SJL and BL/6 experimental groups heavily express Lyve-1 along their lengths.

Significance of Results

This lymphatic vasculature is not noticeably different between strains of mice infected with TMEV, however, the heavily stained confluence of sinuses present in all samples may have some importance in the infection with TMEV. Instead of the easily distinguished vessels observed by Louveau et al.[9], the confluence of sinuses in these mice stained as an indistinct mass. The staining obtained in this experiment is closer in appearance to that obtained by Aspelund et al[10], who also observed diffuse staining in their meninges as well. However, the lymphatic venules in this experiment are still less clearly defined and more difficult to see than their observations. There are no clearly distinguished vessels in this region of the skull, instead, the vessels all run together and cannot be distinguished from one another. As shown in previous

research,[10] the vessels in this region twist and do not form a coherent pattern in this location, so the vessels in this experiment may simply just be so close together that they cannot be distinguished.

An interesting note about the confluence of sinuses in these samples is the strange appearance of some of the sinuses. Particularly shown in Fig. 3a,d,e,g,i,j; the confluence of sinuses in these samples appears almost “stretched out” or distorted from what one would expect the confluence of sinuses to appear. In previous research[9,10], the confluence has appeared to be a small triangular region at the junction of the transverse and sagittal sinuses. Indeed, the confluence of sinuses in Fig. 3b,c,f,h all appear to take this shape. The distortion between the different mice is puzzling, and could be due to a multitude of different factors. One could simply be that the sinuses were distorted upon removal from the skull, and that this caused the distortion seen in this experiment. Another possibility is that the intracranial injection that the mice were given could have caused some sort of distortion in the lymphatic network.

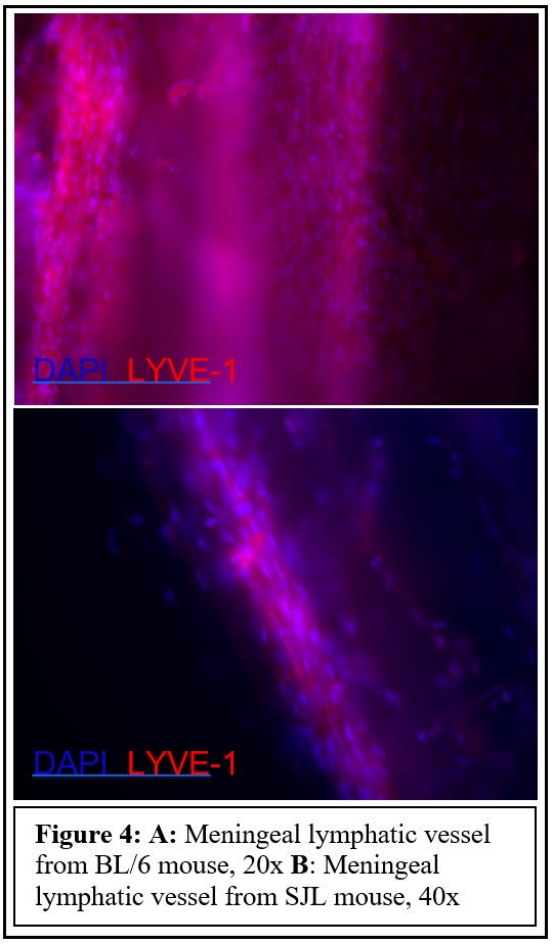

Figure 4: A: Meningeal lymphatic vessel from BL/6 mouse, 20x **B**: Meningeal lymphatic vessel from SJL mouse, 40x

In the infected and non-infected mice, the transverse and sagittal sinuses themselves can be more easily distinguished than the lymphatics in the confluence of sinuses in some of the samples. The outlines of the sinuses can be seen in some of the samples, and do not look very different between the two samples. Both mice expressed Lyve-1 in their meninges at near equal amounts in the same locations, going all the way down the transverse and sagittal sinuses. There is some diffuse staining along these sinuses, and they appear larger and less distinct than in previous research.[9,10] This diffuse appearance could be due to TMEV infection, however, since it is found in the control mice as well, it is more likely due to the difficult nature of staining the meninges.

Fig 4 a,b demonstrates this similarity in expression. Even though the two images are of different magnifications, the similarities of expression between the two strains of mice are similar. Figure 4a shows how diffuse the staining is occasionally, and Fig. 4b demonstrates a closer view of the meningeal lymphatic vessels. At this magnification, the lymphatic cells staining for Lyve-1 can clearly be seen, along with their nuclei. The lymphatic vessels are quite small, with a lumen only a few cells wide, however, they are clearly present in both the BL/6 and SJL mice.

The appearance of the BL/6 and SJL meningeal lymphatic vessels suggests that any lymphangiogenesis that may have occurred was not significant and did not differ between the two groups. Lymphangiogenesis, the process of creating new lymphatic vessels from the outgrowth of old vessels, can be seen after only 48 hours following VEGF-A stimulation.[17] As evidenced in Fig. 3 and Fig. 4, no lymphangiogenesis can be seen surrounding any of the vessels. The confluence of sinuses is stained too diffusely to adequately see the vessels inside, however, since there is no observable difference between the experimental and control groups after 7 days p.i., it is safe to say that lymphangiogenesis likely does not contribute to resistance to TMEV-IDD.

Meningeal CCL21 Expression

Analysis of Meninges

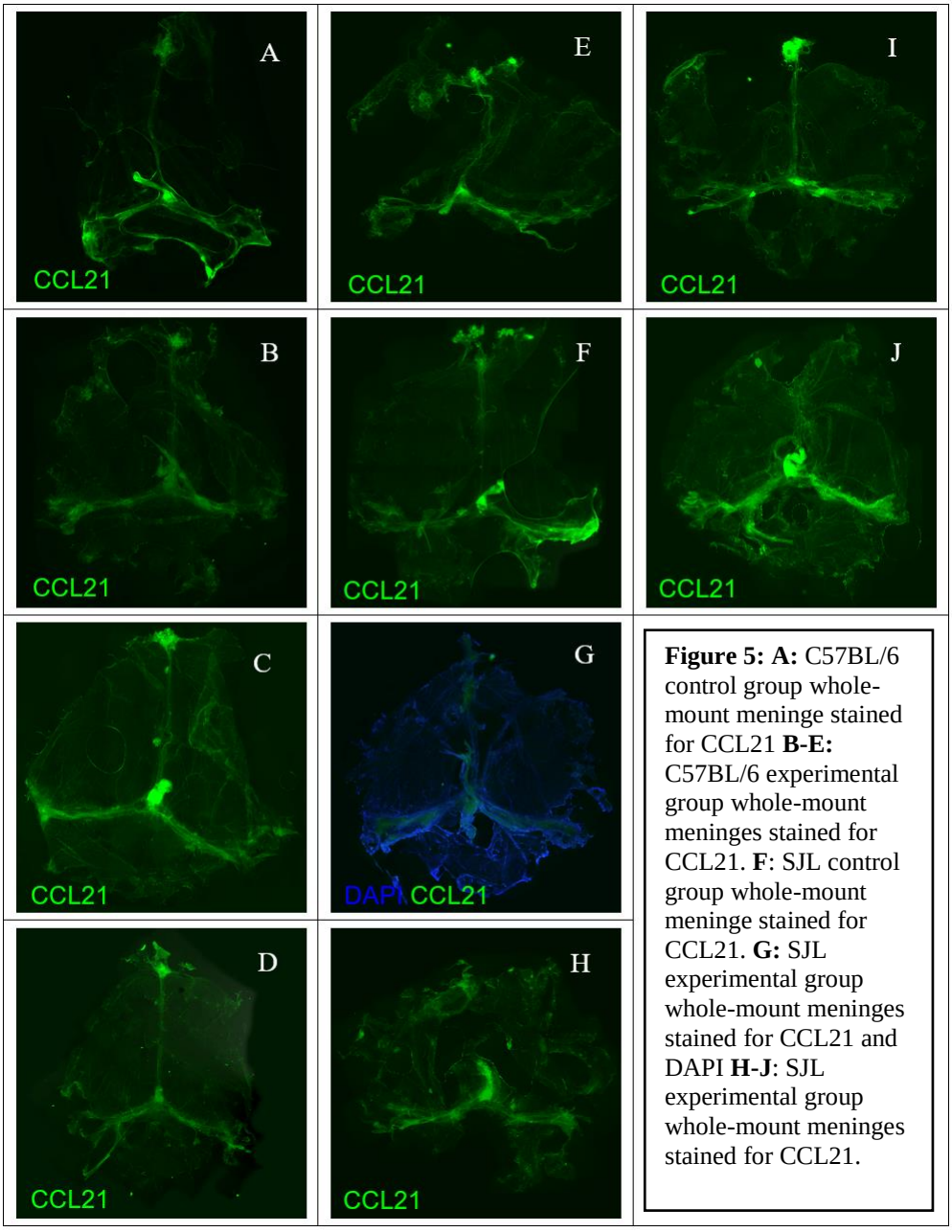

Figure 5: A: C57BL/6 control group whole-mount meninge stained for CCL21 **B-E:** C57BL/6 experimental group whole-mount meninges stained for CCL21. **F**: SJL control group whole-mount meninge stained for CCL21. **G:** SJL experimental group whole-mount meninges stained for CCL21 and DAPI **H-J**: SJL experimental group whole-mount meninges stained for CCL21.

As expected, the meningeal lymphatic systems of both SJL and BL/6 mice expressed CCL21 along both the superior sagittal and transverse sinuses. (Fig. 5a-j) There was also some staining around the edges where the lymphatic venules of these sinuses likely join with the

lymphatic venules at the base of the cranium. These areas stained more intensely and more consistently in both SJL and BL/6 meninges, and are likely due to the increased expression of CCL21 or increased number of lymphatic venules in that area. However, the staining in these areas is diffuse and it is difficult to tell the venules apart.

Additionally, like the Lyve-1 staining, there is also a diffuse mass in the center of each meninge at the confluence of sinuses. This area is typically one of the most intensely stained areas in each meninge, and this is likely due to the large amount of lymphatic tissue in this area. However, the staining in this location is restricted to a smaller area than in most of the Lyve-1 slides. This may suggest that not all the cells in the lymphatic venules express CCL21.

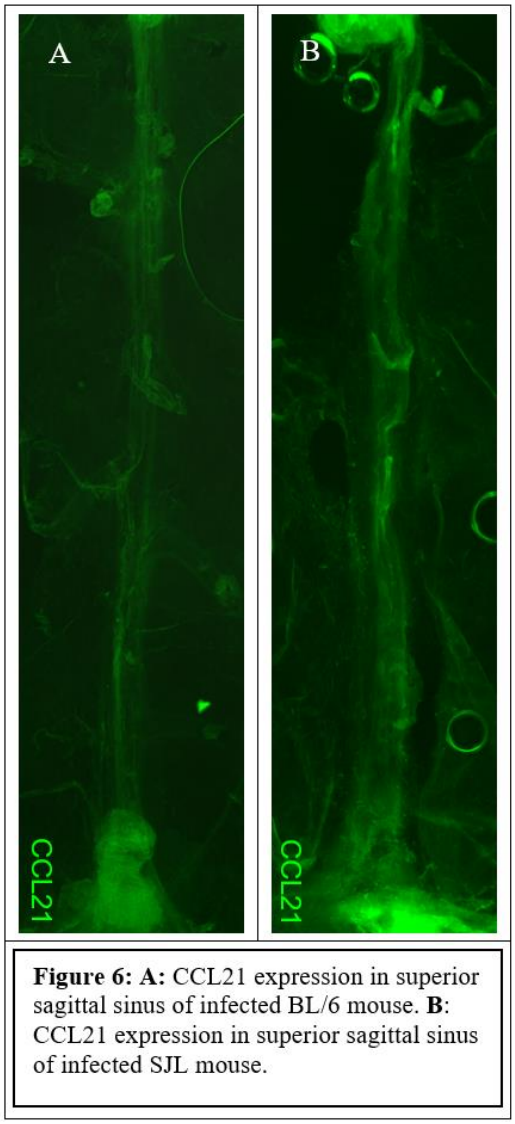

Figure 6: A: CCL21 expression in superior sagittal sinus of infected BL/6 mouse. **B**: CCL21 expression in superior sagittal sinus of infected SJL mouse.

The lymphatic vessel's expression of CCL21 was much more precise than the Lyve-1 expression present in Fig. 3, despite being stained using the same methods and often concurrently. The lymphatic vasculature can be seen much more clearly when visualized using CCL21 staining, even to the point of being able to see distinct lymphatic vessels (Figure 6a,b).

There do seem to be some slight differences between some of the group's meningeal CCL21 expression. As shown in Fig. 6, a BL/6 mouse (Fig. 6a) had weaker staining for CCL21 than the SJL mouse (Fig. 6b). This stronger staining is found in the SJL mice (Fig. 5 a-j)

regardless of staining, however, the difference appears to be more notable in the experimental SJL mice (Fig. 5 g-j) than the experimental BL/6 mice (Fig. 5 b-e). This difference is likely not due to differences in staining technique, as meninges still exhibit this trend even if the SJL and BL/6 meninges were stained at the same time using the same protocol.

Figure 7 demonstrates this difference between the control mice and the experimental mice infected with TMEV. The control mouse (Fig. 7a) shows less significant staining for CCL21 than the infected mouse (Fig. 7b). This difference is not markedly different around the confluence of sinuses, however, it can be seen easily when looking at the transverse sinuses and especially the superior sagittal sinus. The staining is also more diffuse around the vessels in the infected mouse.

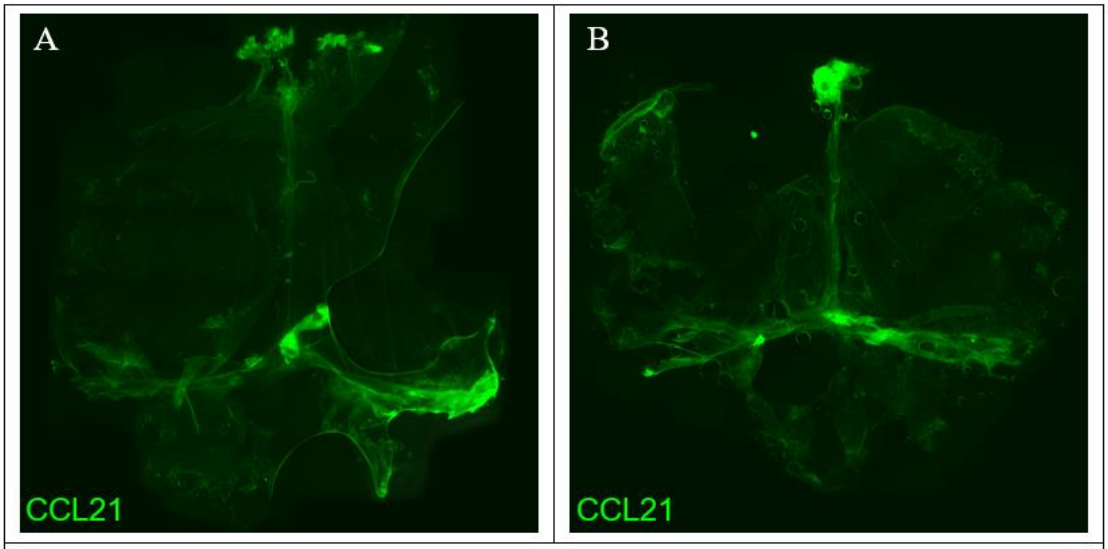

Figure 7: A: whole-mount meninge of SJL control mouse stained for CCL21. **B:** whole mount meninge of experimental SJL mouse infected with TMEV stained for CCL21.

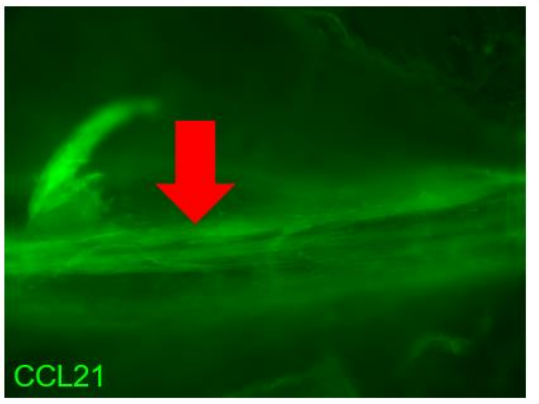

Figure 8: CCL21 expression in control mouse meningeal lymphatic venule, 20x

The structure of the meningeal lymphatic venule shown via CCL21 expression gave clearer images that could be better visualized than those using Lyve-1 (Fig. 4, 8). The red arrow in Fig. 8 points toward one of these vessels, demonstrating a clear expression of CCL21, even in the more weakly stained control mice.

Interestingly, the meninges of the BL/6 mice appeared to be stronger than the meninges of the SJL mice during removal. The SJL meninges were fragile and often seperated during removal. In contrast, the BL/6 meninges appeared to be more intact upon removal, as shown in Fig. 3 and Fig. 5. The differences are especially marked in Fig. 5 due to the brighter staining exhibited by the CCL21 immunofluoresence.

Significance of Results

The more diffuse CCL21 staining in experimental mice (Fig. 7a,b) may be due in part to the nature of the dura and the surrounding tissue. The dura has been shown to leak fluorescent tracers due to its lack of blood-brain barrier properties, and keeps afferent and efferent connections with the dural lymphatic system as well.[18] This leakage could possibly cause some

CCL21 to leak into the dural sinuses, and the increased expression of CCL21 in the dura mater (Fig. 7a,b) could cause this leakage to become more apparent.

CCL21 expression is determined by transmural flow between the lymphatic vessel and the blood vessels, and there is a positive relationship between flow and CCL21 expression along lymphatic vasculature.[19] The increased CCL21 expression shown in these meninges could be the result of increased flow between the meningeal lymphatic vessels and the sinuses, demonstrating that there is more transmural flow in infected SJL mice than infected BL/6 mice.

Treatment of dendritic cells with CCL21 has been shown to enhance the function of dendritic cells by enhancing chemokine expression, which can then influence cytotoxic T lymphocytes and enhance IFN-γ expression and antigen specificity.[20] The early acute phase of the disease has not passed at this point, and in SJL mice this phase of the disease includes increased T cell responses and antibody production.[21] This enhanced immune system activity may be a possible reason why CCL21 expression appears to be more enhanced in infected SJL mice than uninfected SJL mice.

CCL21 has also been shown to be a good chemoattractant for peripheral blood lymphocytes in mice, especially for $CD4^+$ and $CD8^+$ T cells.[22] If CCL21 is expressed more in the meningeal lymphatics of the infected SJL mice than any of the other mice, infected or uninfected, then then this could be significant and may help elucidate the reasons for previous findings. Delayed infiltration of Lyt-2$(CD8)^+$ lymphocytes into the CNS has been shown to be

associated with demyelination in SJL mice, while earlier infiltration into the CNS in BL/6 mice may help clear the virus.[23]

This increased $CD8^+$ cell response could help explain why SJL mice experience the demyelinating disease while BL/6 mice do not. In experiments where mice expressed the P1 region of the TMEV genome, transgenic SJL mice infected with BeAn strain TMEV experienced lower disease incidence and severity, despite having higher viral persistence levels than non-transgenic SJL mice. The transgenic SJL mice also experienced difficulties maintaining self-tolerance.[24] Increasing the $CD8^+$ cell response in the SJL mice could help explain why SJL mice a susceptible to the demyelinating phase of the disease, especially when pairing the increased $CD8^+$ cell response caused by higher CCL21 with delayed infiltration of lymphocytes into the CNS.[23]

Additionally, injection of TMEV-induced $CD8^+$ cells into uninfected SJL mice has been shown to induce clinical signs of TMEV in uninfected mice such as hind limb paralysis and axonal degeneration in the spinal cord.[25] If the increased staining for CCL21 is indeed caused by an increased production of CCL21 in the meningeal lymphatic system, then this could cause an increase in chemotaxis of $CD8^+$ cells into the CNS. The increased concentration of $CD8^+$ cells could theoretically cause an increased amount of damage in the CNS manifesting in the chronic stage of TMEV.

This increase in CCL21 causing a possible increase in $CD8^+$ would contradict previous evidence stating that an increase in $CD8^+$ cells can help protect TMEV-infected mice.[26] This

increase was seen in the results of this experiment, however, the number of $CD8^+$ cells based on CCL21 expression would contradict this finding. Increased CCL21 expression in the meningeal lymphatic vessels and surrounding sinuses is not a definitive sign of an increase in $CD8^+$, however, it is a strong suggestion that there is a higher concentration of $CD8^+$ cells here at 7 days p.i.

SECTION IV

CONCLUSION

The purpose of this experiment was to observe the meningeal lymphatic system during infection with the BeAn strain of Theiler's virus and determine if this system could play a role in determining resistance to the TMEV-IDD that is present in C57BL/6 mice, but not in SJL mice. All experimental mice were successfully infected, and experienced weight loss in accordance with established criteria for infection. Seizures were observed in seven of the eight C57BL/6 mice, and the only mouse that did not seize during observation likely seized before it was observed, since it appeared to be in the post-ictal phase during observation.

Successful extraction of the meninges of each mouse was achieved. One interesting note is that the meninges of the BL/6 mice were stronger and easier to dissect than the SJL meninges. Additionally, the confluence of sinuses in many samples were distorted, either due to dissection technique or some unknown factor. The Lyve-1 expression of the meninges were similar across all mice, regardless of infection status or strain of mouse. There was no consistent difference in Lyve-1 expression, and there was no observable lymphangiogenesis. CCL21 expression appeared higher in the infected SJL mice than any other group, pointing to a possible contributing factor to the demyelinating disease found in SJL mice. The increased CCL21 expression attracts dendritic cells, which can influence cytotoxic T lymphocytes and increase their concentration. This increase in concentration could lead to the clinical symptoms of TMEV-IDD, since injection of TMEV-induced $CD8^+$ cells can induce these symptoms.

These results demonstrate that the meningeal lymphatic system may play a role in the susceptibility of SJL mice to TMEV-IDD. Since there were differences in CCL21 expression between the infected SJL and BL/6 mice, there is likely some role for this difference. Further experiments to clear these problems should focus on using more markers for different cells, such as $CD8^+$ markers or similar. Additionally, spinal and brain sections should be taken on any other SJL mice that exhibit seizures to determine if there are any sources of damage that could have caused them, and mice should be injected in a location other than the confluence of sinuses to determine if this has any effect on the distortion found in this experiment.

REFERENCES

1. Welsh CJ, Steelman AJ, Mi W, Young CR, Dean DD, Storts R. Effects of Stress on the Immune Response to Theiler's Virus – Implications for Virus-Induced Autoimmunity. Neuroimmunomodulation. 2010;17(3):169-172.

2. Zoecklein LJ, Pavelko KD, Gamez J, Papke L, McGavern DB, Ure DR, et al. Direct Comparison of Demyelinating Disease Induced by the Daniel's Strain and BeAn Strain of Theiler's Murine Encephalomyelitis Virus. Brain Pathol. 2003;3(3):291-308.

3. Gilli F, Li L, Pachner R. The immune response in the CNS in Theiler's virus induced demyelinating disease switches from an early adaptive response to a chronic innate-like response. J Neurovirol. 2016; 22(1):66-79.

4. Dal Canto, M.C., Kim, B.S., Miller, S.D., et al. "Theiler's murine encephalomyelitis virus (TMEV)-induced demyelination: a model for human multiple sclerosis." *Methods*, vol. 10, no. 3, 1996, pp. 453-461.

5. Oleszak EL, Leibowitz JL, Rodriguez M. Isolation and characterization of two plaque size variants of Theiler's murine encephalomyelitis virus (DA strain). J Gen Virol. 1988;69(9):2413-2418.

6. Patick AK, Pease LR, David CS, Rodriguez M. Major histocompatibility complex-conferred resistance to Theiler's virus-induced demyelinating disease is inherited as dominant trait in B10 congenic mice. J Virol. 1990;64(11):5570-5576.

7. Abbas AK, Lichtman AH, Pillai S. Basic immunology: Functions and disorders of the immune system. 6th ed. St. Louis: Elsevier; 2016

8. Hong S, Kaer LV. Immune Privilege: Keeping an Eye on Natural Killer T Cells. J Exp Med. 1999;190(9):1197-1200.

9. Louveau A, Smirnov I, Keyes TJ, Eccles JD, Rouhani SJ, Peske D, et al. Structural and functional features of central nervous system lymphatic vessels. Nature. 2015;523:337-341.

10. Aspelund A, Antila S, Proulx ST, Karlsen TV, Karaman S,Detmar M, et al. A dural lymphatic vascular system that drains brain interstitial fluid and macromolecules. J Exp Med. 2015;212(7):991-999.

11. Yoshida R, Imai T, Hieshima K, Kusuda J, Baba M, Kitaura M, et al. Molecular cloning of a novel human CC chemokine EBI1-ligand chemokine that is a specific functional ligand for EBI1, CCR7. J Biol Chem. 1997;272(21):13803-13809.

12. Luo HY, Broux B, Wang XH, Hu Y, Ghannam S, Jin W, et al. EphrinB1 and EphrinB2 regulate T cell chemotaxis and migration in experimental autoimmune encephalomyelitis and multiple sclerosis. Neurobiol Dis. 2016;91(1):292-306.

13. Libbey JE, Kirkman NJ, Smith MC, Tanaka T, Wilcox KS, White HS, et al. Seizures following picornavirus infection. Epilepsia. 2008;49(6):1066-1074.

14. Rodriguez M, Davis CS. Demyelination Induced by Theiler's Virus: Influence of the H-2 Haplotype. J Immunol. 1985;135(3):2145-2148.

15. Racine, RJ. Modification of seizure activity by electrical stimulation: II. Motor seizure. Electroencephalogr Clin Neurophysiol. 1972;32(3):281-294.

16. Steward KAA, Wilcox KS, Fujinami RS, White HS. Theiler's virus infection chronically alters seizure susceptibility. Epilepsia. 2010;51(8):1418-1428.

17. Cursiefen C, Chen L, Borges LP, Jackson D, Cao J, Radziejewski C. VEGF-A stimulates lymphangiogenesis and hemangiogenesis in inflammatory neovascularization via macrophage recruitment. J Clin Invest. 2004; 113(7):1040-1050

18. Engelhardt B, Vajkoczy P, and Weller RO. The movers and shapers in immune privilege of the CNS. Nature Immunol. 2017;18:123-131.

19. Miteva DO, Rutkowski JM, Dixon JB, Kilarski W, Shields JD, Swartz MA. Transmural Flow Modulates Cell and Fluid Transport Functions of Lymphatic Endothelium. Circ Res. 2010;106(5):920-931.

20. Hong CY, Lee HJ, Kim HJ, Lee JJ. The Lymphoid Chemokine CCL21 Enhances the Cytotoxic T Lymphocyte-Inducing Functions of Dendritic Cells. Scan J Immunol. 2014;79(3):173-180.

21. Oleszak EL, Chang JR, Friedman H, Katsetos CD, Platsoucas CD. Theiler's Virus Infection: a Model for Multiple Sclerosis. Clin Microbio Rev. 2004;17(1):174-207.

22. Gunn MD, Tangemann K, Tam C, Cyster JG, Rosen SD, Williams LT. A chemokine expressed in lymphoid high endothelial venules promotes the adhesion and chemotaxis of naïve T lymphocytes. Proc Natl Acad Sci USA. 1998;95(1):258-263.

23. Lindsely MD, Rodriguez M. Characterization of the inflammatory response in the central nervous system of mice susceptible or resistant to demyelination by Theiler's virus. J Immunol, 1989;142(8):2677-2682.

24. Myoung J, Bahk YY, Kang HS, Dal Canto MC, Kim BS. Anticapsid Immunity Level, Not Viral Persistence Level, Correlates with the Progression of Theiler's Virus-Induced Demyelinating Disease in Viral P1-Transgenic Mice. J Virol. 2008;82(11):5606-5617.

25. Libbey JE, Cusick MF, Tsunoda I, Fujinami RS. Antiviral $CD8^+$ T cells cause an experimental autoimmune encephalomyelitis-like disease in naïve mice. J. Neurovirol. 2012;18(1):45-54.

26. Borrow P, Tonks P, Welsh CJR, Nash AA. The role of $CD8^+$ T cells in the acute and chronic phases of Theiler's murine encephalomyelitis virus-induced disease in mice. J Gen Virol. 1992;72:1861-1865.